Available online at www.sciencedirect.com
ScienceDirect
Journal of Nuclear Materials 359 (2006) 202–207
journal of nuclear materials
www.elsevier.com/locate/jnucmat

Residual stress measurements on a stress relieved Zircaloy-4 weld by neutron diffraction

D.G. Carr [a,*], M.I. Ripley [a], D.W. Brown [b], S.C. Vogel [b], T.M. Holden [c]

[a] *Australian Nuclear Science and Technology Organisation, PMB 1 Menai 2234, NSW, Australia*
[b] *Los Alamos National Laboratory, Los Alamos, NM 87545, USA*
[c] *Northern Stress Technologies, Deep River, Ont., Canada K0J 1P0*

Received 25 October 2005; accepted 29 August 2006

Abstract

The macroscopic stress distribution across an annealed Zircaloy-4 gas tungsten arc weld was measured by neutron time-of-flight diffraction at the SMARTS diffractometer at Los Alamos National Laboratory. The stresses after annealing are about 40% lower than those in the same weld prior to heat treatment. The intergranular strains in the reference coupons, which give the macroscopic stress free lattice spacings, are consistent with the difference in cooling the strongly textured plate and the weakly textured weld.

1. Introduction

The reactor vessel for the new Australian replacement research reactor is constructed from Zircaloy-4 plates that are welded together. The residual stresses in a butt weld representative of those made by the tungsten inert gas method for the reactor vessel were reported recently [1]. A longitudinal stress extending into the parent plate material with a maximum value of 220 ± 50 MPa was observed with balancing longitudinal compressive stresses far from the weld. A small transverse stress of 60 ± 50 MPa was noted in the vicinity of the weld. Rapid changes of texture were noted on passing from the marked texture of the parent plate to the weak texture in the heat-affected zone and the weld metal.

After manufacture and before service in the reactor a weld would be given a stress-relieving heat treatment at 748 K for 30 min. The purpose of this short paper is to report the results of a similar stress-relieving heat treatment on the as-welded plate tested previously [1] since these are of technical interest. The set-up for the neutron diffraction experiments is the same as used previously. Measurements were made on the stress-relieved intact weld and on stress-relieved reference samples. These had been cut previously from various locations in the plate and the weld. In Ref. [1] there was no discussion of the origin of the strains in the reference samples. The present measurements suggest that the differences in strain between the weld and the parent plate coupons basically originate in the

* Corresponding author. Tel.: +61 2 9717 3504; fax: +61 2 9543 7179.
E-mail address: dgc@ansto.gov.au (D.G. Carr).

0022-3115/$ - see front matter Crown Copyright © 2006 Published by Elsevier B.V. All rights reserved.
doi:10.1016/j.jnucmat.2006.08.021

difference between cooling a textured and non-textured polycrystalline aggregate.

2. Theory

Measurements of residual strain by white-beam time-of-flight diffraction make use of Bragg's law

$$\lambda_{hkil} = 2\, d_{hkil} \sin\theta. \quad (1)$$

The neutron counters are in fixed positions around $2\theta = \pm 90°$. The wavelength of the neutrons, λ_{hkil}, from diffracting planes $\{hkil\}$ is directly proportional to their time-of arrival in the counter and the constant of proportionality is determined by diffraction from a standard powder of CaF_2. Care was taken to ensure that the samples were centered on the diffractometer [2].

The determination of strain from the measured lattice spacings requires the knowledge of reference lattice spacings, d^0_{hkil}

$$\varepsilon_{hkil} = (d_{hkil} - d^0_{hkil})/d^0_{hkil}. \quad (2)$$

The reference lattice spacings were obtained from coupons cut from eight positions in the plate and the weld. The action of cutting destroys the macroscopic stress field but any changes in lattice spacing due to chemistry or type-2 stresses remain. The difference between the intact weld and the coupon gives the strain corresponding to the stress field of interest.

It was assumed that the principal directions of the stress field were longitudinal, L, parallel to the weld and parallel to the rolling direction in the plate, transverse to the weld in the plane of the plate, T, and normal to the plate, N. The asymmetric weld preparation could well lead to principal stresses that are rotated away from the longitudinal and transverse directions. In addition it was shown in [1] that the distribution of stresses and of intensity of the diffraction peaks was displaced from the centre of the weld cap in the as-welded state. In this case the asymmetry and shift were ascribed primarily to the fact that the welding torch was not held normal to the plate surface. There may also be a contribution from the asymmetric set-up of the plate. Investigation of this effect, whose magnitude is difficult to establish a priori, will be the subject of future work.

The macroscopic longitudinal strains, determined from single peak fits of the various reflections, $\{hkil\}$, at a given location are given in terms of the unique stress field, σ^L, σ^T, σ^N, at the location as follows:

$$\varepsilon^L_{hkil} = \{\sigma^L - \nu_{hkil}(\sigma^T + \sigma^N)\}/E_{hkil}. \quad (3)$$

Similar equations hold for the other directions. E_{hkil} and ν_{hkil} are the diffraction elastic constants for the {hkil} reflection calculated as a function of position with the aid of the elasto-plastic self-consistent (EPSC) model [3] using the appropriate texture measured in parent and weld locales [1]. The diffraction elastic constants are given in Table 1 of [1] for the case of the parent plate (fairly strong texture) and the weld (weak texture). The single crystal, that is unconstrained, elastic constants for Zr are E_{0002} and $E_{10.0}$ are 125.3 and 97.4 GPa, respectively. The constraint provided by the surrounding grains reduces Young's modulus by 15% for the elastically stiff [0002] direction but by less than 1% on the elastically softer [10.0] and [11.0] directions. It is therefore necessary to include texture in order to obtain accurate estimates of Young's modulus, though the degree of texture is of secondary importance as Table 1 of Ref. [1] shows.

Given a stress along a crystallographic direction, say [10.0], the perpendicular response for the polycrystalline case is an average, weighted by the texture, of directions perpendicular to the [10.0] direction. The values in Table 1 for ν_{hkil} are different by as much as 15% between the parent plate and the weld. The values calculated with the EPSC for random texture are in good agreement with the Kröner model which also assumes random texture. The perpendicular single crystal response when the stress is applied along the [10.0] direction varies from 0.240 in the [0002] direction to 0.396 for the [11.0] direction, a 65% change. The presence of constraining grains in the polycrystal clearly should be taken into account. Just as the spread in values of the perpendicular single crystal response is more marked than the parallel response so the constrained values of ν_{hkil} show more variation between the plate and the weld.

It is therefore important to use the values of the diffraction elastic constants for the weld texture in the weld and the parent texture outside the HAZ. The locations in the HAZ where the texture is strong but different to the parent plate in the region centered on 4–5 mm from the weld centre may have a systematic error. If it is assumed that ν_{hkil} is higher by 0.045, which is the maximum difference between the weld and the parent, this increases the

Table 1
Thermal strains (10^{-4}) in Zr-4 on cooling from 900 K to 293 K calculated from the EPSC model for a number of reflections in the strongly textured plate and the weakly textured weld

hkil	Plate			Weld			Relative difference (W–P)		
	L	*T*	*N*	*L*	*T*	*N*	*L*	*T*	*N*
$\{10\bar{1}0\}$	−0.3	−3.2	−7.8	−3.8	−3.9	−3.6	−3.5	−0.7	4.2
$\{10\bar{1}1\}$	2.1	−0.5	−5.2	−1.2	−1.4	−0.8	−3.3	−0.9	4.4
$\{10\bar{1}3\}$	7.6	4.9	0.3	4.1	4.0	4.4	−3.5	−0.9	4.1
$\{11\bar{2}0\}$	−0.3	−3.2	−7.8	−3.8	−3.9	−3.6	−3.5	−0.7	4.2
$\{11\bar{2}2\}$	2.5	0.0	−5.1	−0.8	−0.9	−0.9	−3.3	−0.9	4.2
$\{0002\}$	10.3	7.6	3.3	7.1	7.0	7.3	−3.2	−0.6	4.0

value of all the stress components by about 20 MPa. This is half the uncertainty postulated for the stresses. This is likely to be the maximum shift that could occur in the HAZ. Since the root mean square difference in ν_{hkil} between the weld and the plate is 0.026 a shift of about 15 MPa is more appropriate.

The values of σ^L etc. were found by weighted least squares regression fitting Eq. (3) to about fifty measured strains of the 17 different *hkil* measured in the three directions at each location in the weld. Weights were estimated using the uncertainty from the calculation of the single peak fits for each *hkil*. After fitting, the validity of the fit was checked by taking the weighted residuals of the complete strain data set and testing against an assumption of normality. The weighted residuals where found to have a normal probability plot correlation coefficient of 0.98.

3. Experiments

3.1. Samples

The butt weld consisted of two 8.6 mm thick plates of hot-rolled and annealed Zr-4 joined by gas (Ar 5–20% He) tungsten arc welding: details of the manufacture are given in reference [1]. A neighboring segment was wire-cut into 2 mm slices through the thickness of the plate parallel to the weld at many locations in the plate, the heat affected zone and the weld metal. These slices were further cut into $2 \times 2 \times 2\ \mathrm{mm}^3$ cubes and re-assembled into $4 \times 4 \times 4\ \mathrm{mm}^3$ reference coupons preserving the orientation of the original cubes. The weld and the references were given the following stress-relieving heat-treatment. The material was heated in air from room temperature to 473 K at 400 °C/h, from 473 K to 748 K at 50 °C/h and held at 748 K for 30 min and allowed to cool to room temperature in the furnace. No β-phase was expected or observed in the experiments.

3.2. Neutron diffraction

The measurements were made with the SMARTS time-of-flight diffractometer [4] at the Los Alamos Neutron Scattering Center (LANSCE) at Los Alamos National Laboratory. The diffractometer was set up for strain scanning with a small incident neutron beam and radial collimators of 2 mm horizontal width in the diffracted beams. For the transverse and normal measurements the beam-defining incident slit was 2 mm wide and 25 mm high. For the longitudinal and normal measurements the height of the slit was restricted to 2 mm since there is a gradient of longitudinal strain perpendicular to the weld. The count times taken for the transverse and longitudinal measurements were 0.5 h and 2 h, respectively. Eight reference samples were mounted on small pillars, carefully centred with the aid of the odolites to a precision of ±0.1 mm, and measured in the longitudinal, transverse and normal directions.

4. Results and discussion

4.1. Annealed weld

The measured macroscopic stresses after stress-relieving by annealing are shown in Fig. 1 as a function of position across the weld for the longitudinal, transverse and normal directions by solid circles. For comparison, the results in the as-welded condition are shown by open circles. The form of the distribution is unchanged by the heat treatment but the magnitude of the longitudinal stress has been reduced by about 40% from 220 ± 50 MPa to 140 ± 50 MPa. A balancing compressive longitudinal stress is observed in the plate far from the weld. The transverse stress is reduced from about 60 MPa

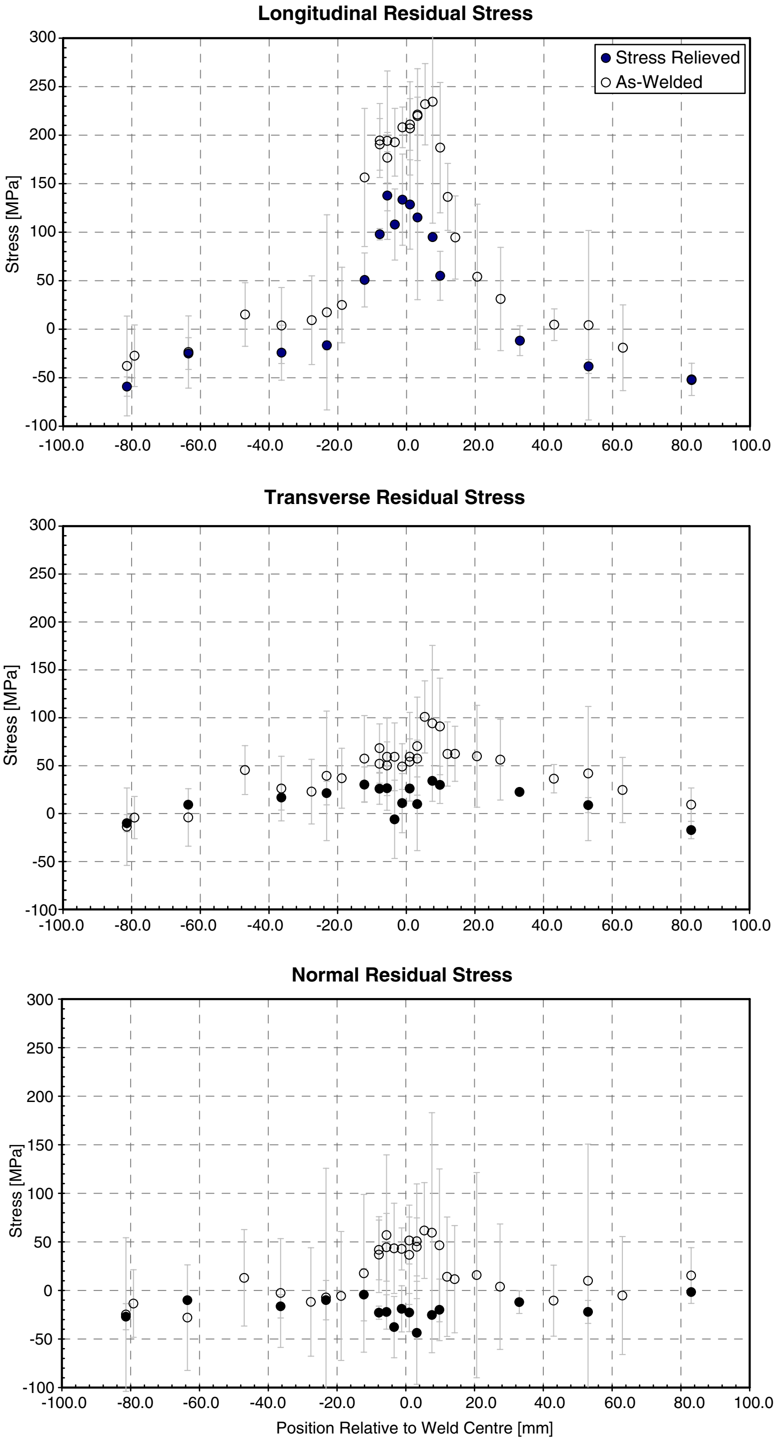

Fig. 1. Variation of the macroscopic residual stresses in a Zr-4 weld after a stress-relieving heat-treatment (filled circles) and as-welded (open circles). The as-welded stresses are reduced by about 40% by the heat treatment. Measurements were taken across the plate at the mid-thickness position as indicated on the scaled drawing of the plate and weld geometry parallel to the weld direction (*L*), transverse to the weld in the plane of the plate (*T*) and normal to the plate (*N*).

to about 30 MPa which is below one standard deviation. The normal stress appears to be offset at all locations by −20 MPa, which again is less than one standard deviation.

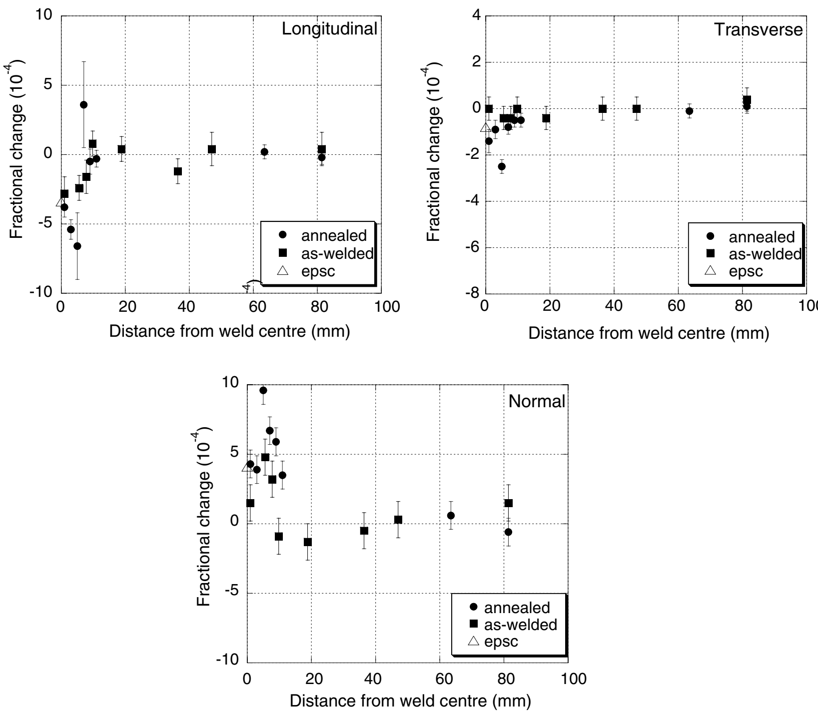

Fig. 2. Variation of the $\{10\bar{1}1\}$ lattice spacing of coupons cut from the Zr-4 weld as a function of the distance from the centre of the weld. Results are shown for the as-welded and as-annealed states in the longitudinal (parallel to the weld direction and to the rolling direction of the parent plate), transverse to the weld in the plane of the plate and the plate normal directions. The variation is expressed relative to the value at the edge of the plate. Calculations of the change in thermal intergranular strain in the EPSC model between plate texture and weld texture are shown as triangles and are consistent with the measurements.

One of the concerns in α-phase Zr-alloy welds is the often-observed re-orientation of [0002] poles in the heat-affected zone [5,6] from longitudinal or normal directions in the parent plate to the transverse direction. In this region, tensile strains in [0002] grains can provide a preferred location of reduced potential energy for hydrogen atoms in solution that may eventually precipitate as zirconium hydrides. The region where this effect occurs in our weld is between ±(4–6) mm from the weld centre. In this region the macroscopic stress in the transverse direction is about +30 MPa and the longitudinal stress is +140 MPa. The expected thermal intergranular stress for [0002] grains from an EPSC calculation and experiment [7] is +70 MPa so the sum of the intergranular and microscopic stresses for [0002] grains oriented transverse to the weld is about 100 MPa.

4.2. Reference samples

No discussion was given in [1] of the behavior of the reference lattice spacings as a function of position through the weld. The variation of the $\{10\bar{1}1\}$ lattice spacing of the reference coupons is shown in Fig. 2 as a function of distance from the centre of the weld. The lattice spacing is expressed as the fractional change with respect to the value at the edge of the plate. Results are shown for both the as-welded and as-annealed reference coupons, which superpose on each other. The lattice spacing for the other reflections shows the same changes in the three directions. Note that there is a decrease in the longitudinal direction and an increase in the normal direction and very little change in the transverse direction as the weld is approached. The variation was initially hard to understand but the EPSC gave a quantitative explanation.

The crystallographic texture in the parent plate [1] is such that, in the longitudinal direction, $\langle 10\bar{1}0\rangle$, $\langle 21\bar{3}0\rangle$ and $\langle 11\bar{2}0\rangle$ poles are strongly preferred resulting in the absence of $\langle 0002\rangle$ poles in that direction. The reverse is true in the normal direction and in the transverse direction the distribution of intensity is nearly uniform. The crystallographic texture is weak [1] in the weld region. The thermal strains may be calculated confidently in the EPSC model since only elasticity is involved and the reference coupons can be assumed to be free from macroscopic stress. The thermal strains were calculated for the measured plate and weld texture [1] using the pure Zr single crystal coefficients of thermal expansion of 5.8×10^{-6} and 10.3×10^{-6} K^{-1} for the a and c directions, respectively [8]. A selection of results is shown in Table 1. The calculated thermal strains in the weld relative to the parent plate are compressive for the longitudinal direction (-3.3×10^{-4}), tensile for the normal direction ($+4.2 \times 10^{-4}$) and slightly compressive for the transverse direction (-0.7×10^{-4}). To a first approximation, for the transverse direction where the plate texture is near random, the thermal strains are nearly the same as in the random case. The results of the EPSC thermal strain calculation are shown as open triangles in Fig. 2 and give a quantitative explanation of the behavior. Note that for a given sample direction the EPSC predicts that all reflections, $hkil$, show the same relative strain between the weld and the plate.

It might have been expected that the weld region would experience some plastic deformation and that this might strongly influence the intergranular strains. The thermal calculation was repeated but with the addition of a 0.2% plastic deformation after cooling for the case of the weld texture. The relative strains were then -0.7×10^{-4} (L), $+3.1 \times 10^{-4}$(N) and -2×10^{-4}(T) and these are in worse agreement with observation than the simple thermal calculation. Since both the as-welded and as-annealed reference strains were identical, the as-welded references never exhibited intergranular strains arising from plastic deformation and only thermal strains were present even in the as-welded state. The 40% reduction in the macroscopic stress field is not paralleled in the intergranular effects but this is not expected.

It is also worth noting the experimental fact that that lattice spacings of the annealed reference samples were usually within a relative uncertainty of 3×10^{-4} of the as-welded values in the two sets of measurements taken one year apart; indicating that the alignment was executed carefully and the calibration was accurate.

5. Conclusions

The maximum longitudinal stress in the weld was lowered from 220 to 140 MPa after a heat-treatment at 748 K while the transverse stress was reduced below the level of the experimental uncertainty ($\pm$50 MPa). The values of the reference strains in the weld were consistent with thermal strains generated by cooling the weakly textured weld region.

Acknowledgements

We wish to acknowledge the experimental assistance of T. Sisneros, and the use of the EPSC code of Carlos Tomé. LANSCE is a national user facility funded by the United States Department of Energy, Office of Basic Science, under contract number W-7405-ENG-36 with the University of California. This research was jointly funded through ANSTO projects 0045 m and 0154 m.

References

[1] D.G. Carr, M.I. Ripley, T.M. Holden, D.W. Brown, S.C. Vogel, Acta mater. 52 (2004) 4083.
[2] X.-L. Wang, Y.D. Wang, J.W. Richardson, J. Appl. Cryst. 35 (2002) 533.
[3] P.A. Turner, C.N. Tomé, Acta metall. mater. 42 (1994) 4143.
[4] M.A.M. Bourke, D.C. Dunand, E. Ustundag, Appl. Phys. 75 (2002) 1.
[5] C.E. Coleman, G.L. Doubt, R.W.L. Fong, J.H. Root, J.W. Bowden, S.Sagat and R.T. Webster, Proc. 18th Int. Symp. on Zirconium in the Nuclear Industry, ASTM Standard Technical Publication 1245 p264 (American Society for Testing and Materials, Philadelphia, PA,1994).
[6] J.H. Root, C.E. Coleman, J.W. Bowden, M. Hayashi, J. Pressure Vessel Technol. 119 (1997) 137.
[7] J.W.L. Pang, T.M. Holden, P.A. Turner, T.E. Mason, Acta mater. 47 (1999) 373.
[8] C.N. Tomé, N. Christodoulou, P.A. Turner, M.A. Miller, C.H. Woo, J.H. Root, T.M. Holden, J. Nuclear Mater. 227 (1996) 237.